



An azo-azomethine ligand and its copper(II) complex: Synthesis, X-ray crystal structure, spectral, thermal, electrochemical and photoluminescence properties



Tugba Eren^a, Muhammet Kose^a, Nurcan Kurtoglu^b, Gokhan Ceyhan^a, Vickie McKee^{c,d}, Mukerrem Kurtoglu^{a,*}

^a Department of Chemistry, Kahramanmaraş Sutcu Imam University, Kahramanmaraş 46050, Turkey

^b Department of Textile Engineering, Kahramanmaraş Sutcu Imam University, Kahramanmaraş 46050, Turkey

^c Department of Chemistry, Loughborough University, Leicestershire LE11 3TU, UK

^d School of Chemical Sciences, Dublin City University, Glasnevin, Dublin 9, Ireland

ARTICLE INFO

Article history:

Received 17 November 2014

Received in revised form 10 February 2015

Accepted 5 March 2015

Available online 26 March 2015

Keywords:

Azo-azomethine
Copper complex
Crystal structure
Spectroscopic studies
Electrochemistry
Photoluminescence

ABSTRACT

In this study, a new azo-azomethine ligand, 4-[(*E*)-phenyldiazenyl]-2-[(*E*)-{[4-(propan-2-yl)phenyl]imino}methyl]phenol (*HL*) and its Cu(II) complex, [CuL₂] were synthesized and characterized by the analytical and spectroscopic methods such as elemental analyses, FT-IR, ¹H, ¹³C NMR and mass spectra. Molecular structures of the ligand and its Cu(II) complex were determined by single crystal X-ray diffraction studies. In the structure of the ligand, there is an intramolecular phenol-imine hydrogen bond (O1...N1) with a distance of 2.580(3) Å. There are also intermolecular hydrogen bond type interactions CH...O and CH...N=N stabilizing the structure. The crystal structure of the Cu(II) was solved in the *triclinic* space group *P* $\bar{1}$. In the structure of the complex, the Cu(II) ion is four coordinate bonded to two phenolate oxygens and two imine nitrogens of two ligand molecules in an approximate square-planar geometry. The Cu–O bonds are in *trans* configuration. Thermogravimetric data revealed that the Cu(II) complex is thermally more stable than the azo-azomethine compound (*HL*). Upon coordination with Cu(II) ion, both excitation and emission intensities of the ligand shifted to lower values.

© 2015 Elsevier B.V. All rights reserved.

1. Introduction

Azo compounds, containing two phenyl rings separated by an azo (–N=N–) bond, are versatile molecules and have received much attention in both fundamental and applied research areas. Azo dyes have been widely used in many practical applications such as coloring fibers [1], photoelectronics [2], printing systems [3], optical storage technology [4,5], textile dyes [6,7] as well as in many biological reactions [8,9] and in analytical chemistry [10,11]. Both Schiff bases and azo compounds are also important structures in medicinal and pharmaceutical fields and it has been suggested that the azomethine linkage might be responsible for the biological activities displayed by Schiff bases [12]. These compounds have also received special attention because of their mixed soft–hard donor characters, versatile coordination behavior, optical and pharmacological properties and thermal properties.

* Corresponding author. Tel.: +90 344 280 1450; fax: +90 344 280 1352.

E-mail addresses: kurtoglu01@gmail.com, mkurtoglu@ksu.edu.tr (M. Kurtoglu).

In the last few decades many copper complexes have been reported [13,14]. The growing interest on the coordination compounds of copper with various *N*-donor ligands, comes mainly from their capability of combining characteristic structural flexibility [13,14], mimicking of protein active sites [15–17], ease of preparation [18,19], and stabilization of both oxidation states of the metal usual in biological systems [20,21]. Considerable interest in various *N* and *O* donor ligands especially Schiff bases and their transition metal complexes have also grown in the areas of chemistry and biology due to biological activities, such as antiviral [22,23], antitumor [24,25], bactericidal [26,27], fungicidal [18] and nonlinear optical properties [28,29]. This type of the compounds have been used for metal analyses, for device applications related to telecommunications, optical computing [30,31], storage [32,33], and information processing [34,35]. The redox potential of copper complexes with various *N* and *O*-donor ligands has deserved a strong interest since it seems to be directly related to some of the biologically important properties of this type of compounds. Additionally, many of Schiff bases exhibit tautomeric rearrangements because of intramolecular proton transfer

between the enolimine (OH) and the ketonamine (NH) forms possessing different electronic absorption spectra. X-ray single-crystal diffraction is a very powerful tool to investigate tautomerisms because it provides detailed information on molecular conformation and supramolecular interactions in the solid state. The tautomerism of azomethines received considerable interest due to application of improved experimental and theoretical methods. Recently, some azo-azomethines and their metal chelates have been reported [36–39]. In our previous work, 4-[(*E*)-phenyldiazanyl]-2-[(*E*)-(phenylimino)methyl]phenol and 2-[(*E*)-(2-hydroxy-5-methylphenyl)imino]methyl-4-[(*E*)-phenyldiazanyl]phenol compounds were synthesized and structurally characterized [40,41].

Because of the importance of azo-azomethine compounds and in continuance of our interest in the synthesis of azo-azomethine compounds and their transition metal complexes, a novel azo-azomethine ligand, 4-[(*E*)-phenyldiazanyl]-2-[(*E*)-{4-(propan-2-yl)phenyl}imino]methyl]phenol and its Cu(II) complex were prepared and characterized by spectroscopic and analytic methods. Molecular structures of the ligand and its Cu(II) complex were also determined by single crystal X-ray diffraction studies. Thermal studies of the compounds were performed under nitrogen atmosphere in the temperature range of 20–1000 °C. Electrochemical and photoluminescence properties of the synthesised compounds were also investigated.

2. Experimental

2.1. Chemicals

All reagents and solvents for the synthesis and analysis were purchased from commercial sources and used as received unless otherwise noted.

2.2. Physical measurements

NMR spectra were performed using a Bruker Advance 400 MHz. Spectrometer. Mass spectra were recorded on a Thermo Fisher Exactive + Triversa Nanomate mass spectrometer. The FT-IR spectra were obtained (4000–400 cm⁻¹) using a Perkin Elmer spectrum 100 spectrophotometer. Carbon, hydrogen and nitrogen elemental analyses were performed with a model CE-440 elemental analyzer. Thermogravimetric analyses were done on a Perkin Elmer Diamond TG/DTA (Technology by SII) under nitrogen atmosphere with a heating rate of 20 °C/min. Melting points were obtained with a Electrothermal LDT 9200 Apparatus in open capillaries. Cyclic voltammograms were recorded on a Iviumstat Electrochemical workstation equipped with a low current module (BAS PA-1) recorder. The electrochemical cell was equipped with a BAS glassy carbon working electrode (area 4.6 mm²), a platinum coil auxiliary electrode and a Ag/AgCl reference electrode filled with tetrabutylammonium tetrafluoroborate (0.1 M) in DMF and CH₃CN solution and adjusted to 0.00 V versus SCE. Cyclic voltammetric measurements were performed at room temperature in an undivided cell (BAS model C-3 cell stand) with a platinum counter electrode and an Ag/AgCl reference electrode (BAS). All potentials are reported with respect to Ag/AgCl. The solutions were deoxygenated by passing dry nitrogen through the solution for 30 min prior to the experiments, and during the experiments the flow was maintained over the solution. Digital simulations were performed using DigiSim 3.0 for windows (BAS, Inc.). Experimental cyclic voltammograms used for the fitting process had the background subtracted and were corrected electronically for ohmic drop. The single-photon fluorescence spectra of the azo-aldehyde (a), azo-azomethine ligand *HL* and its Cu (II) complex

[CuL₂] were collected on a Perkin Elmer LS55 luminescence spectrometer. All samples were prepared in spectrophotometric grade solvents and analyzed in a 1 cm optical path quartz cuvette.

Data for the ligand and its copper(II) complex were collected at 150(2) K on a Bruker ApexII CCD diffractometer using Mo K α radiation ($\lambda = 0.71073 \text{ \AA}$). Data reduction was performed using Bruker SAINT [42]. SHELXTL was used to solve and refine the structures [43].

2.3. Synthesis of 2-hydroxy-5-[(*E*)-phenyldiazanyl]benzaldehyde (a)

The azo-aldehyde compound 2-hydroxy-5-[(*E*)-phenyldiazanyl]benzaldehyde (a) was prepared according to the published papers [40,41].

2.4. Synthesis of 4-[(*E*)-phenyldiazanyl]-2-[(*E*)-{4-(propan-2-yl)phenyl}imino]methyl]phenol, (*HL*)

The azo-azomethine ligand (*HL*) was prepared according to the known condensation method. 4-Isopropylaniline (0.135 g, 10 mmol) and 2-hydroxy-5-[(*E*)-phenyldiazanyl]benzaldehyde (a) (0.226 g, 10 mmol) were dissolved in 30 mL MeOH. The solution was refluxed for 2 h and then cooled to room temperature. Upon cooling, the azo-azomethine ligand was obtained as red-orange microcrystals which were filtered off, washed with cold MeOH and dried in air. X-ray quality crystals of the ligand were obtained by slow evaporation of the methanol solution.

Yield: 0.146 g (42.5%). m.p.: 139–140 °C. *Anal. Calc.* for C₂₂H₂₁N₃O: C, 76.94; H, 6.16; N, 12.24. Found: C, 76.28; H, 5.97; N, 11.96%. IR (KBr, cm⁻¹): 3320 (OH), 3050 (aromatic), 2957 (C–H), 1616 (C=N). ¹H NMR (CDCl₃ as solvent, γ in ppm): 1.32 (d, CH₃², $J = 6.93 \text{ Hz}$), 2.99 (st, CH₃³, $J = 6.93 \text{ Hz}$), 7.17 (d, aromatic CH¹³, $J = 6.13 \text{ Hz}$), 7.31 (d, aromatic CH¹⁴, $J = 6.13 \text{ Hz}$), 7.33 (d, aromatic CH^{5,9}, $J = 8.45 \text{ Hz}$), 7.35 (s, aromatic CH¹⁶), 7.49 (t, aromatic CH²⁰, $J = 6.76 \text{ Hz}$), 7.56 (t, aromatic CH^{19,21}, $J = 7.37 \text{ Hz}$), 8.04 (d, aromatic CH^{6,8}, $J = 8.45 \text{ Hz}$), 8.07 (d, aromatic CH^{18,22}, $J = 7.37 \text{ Hz}$), 8.78 (s, 1H, –CH¹⁰=N–), 14.06 (b, 1H, –OH). ¹³C NMR (CDCl₃ as solvent, γ in ppm): 24.02 (C¹, C²), 33.83 (C³), 118.17 (C¹³), 119.00 (C¹¹), 121.15 (C⁶, C⁸), 122.61 (C¹⁶), 127.36 (C¹⁴), 127.53 (C⁵, C⁹), 127.78 (C¹⁹, C²¹), 130.56 (C²⁰), 145.53 (C¹⁵), 148.47 (C⁴), 152.63 (C⁷), 161.19 (C¹⁷), 164.18 (C¹²), 164.23 (C¹⁰). ESI mass (m/z): 239 [M–C₆H₉], 263 [M–C₆H₉]⁺, 344 [M+H]⁺, 366 [M+Na]⁺, 686 [2M]⁺, 709 [2M+Na]⁺.

2.5. Synthesis of the Cu(II) complex [CuL₂]

The complex [CuL₂] was synthesized by a general method. To a hot solution of *HL* ligand (0.250 g, 0.73 mmol) in 35 mL CHCl₃ was added 1/2 equivalent amount of copper(II) acetate (0.073 g, 0.37 mmol) in 25 mL CHCl₃ and 20 mL EtOH. The mixture was refluxed for 3 h and then cooled. A brown-red precipitate formed was collected by filtration, washed with cold water and MeOH and dried under vacuum. The brown single crystals of the complex were obtained by slow evaporation of the chloroform solution.

Yield: 0.250 g. (91%). m.p.: 267–268 °C. *Anal. Calc.* for C₄₄H₄₀CuN₆O₂: C, 70.62; H, 5.39; N, 11.23. Found: C, 70.13; H, 5.33; N, 10.54%. IR (KBr, cm⁻¹): 3065 (C–H aromatic), 2956, 2921 (C–H isopropyl), 1611 (C=N), 1595 (C=C), 1471 (N=N), 1379 (C–N), 1341 (C–O), 589 (Cu–O), 462 (Cu–N). ESI mass (m/z): 770 [C₄₄H₄₀CuN₆O₂+Na]⁺, 538 [C₃₂H₃₁CuN₂O₂–1]⁺, 468 [C₂₇H₂₁CuN₂O₂–1]⁺, 344 [C₁₇H₁₇CuN₂O₂]⁺, 308 [C₂₃H₁₇CuN₂O₂+1]⁺.

2.6. X-ray structure solution and refinement

The structures were solved by direct methods and refined on F^2 using all the reflections [43]. All the non-hydrogen atoms were

Table 1
Crystallographic data of the ligand and its Cu(II) complex.

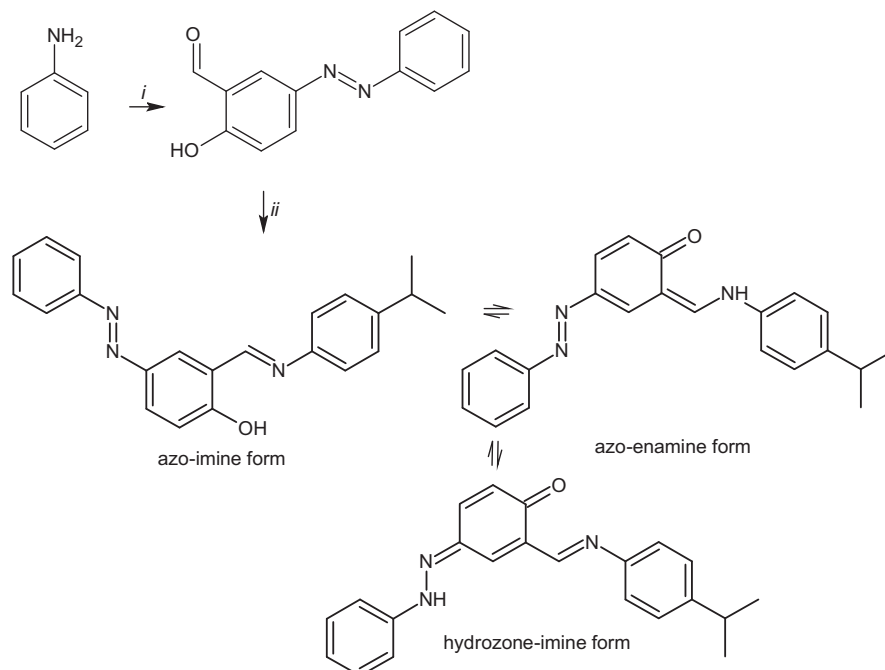
Identification code	<i>HL</i>	[CuL ₂]
Empirical formula	C ₂₂ H ₂₁ N ₃ O	C ₄₄ H ₄₀ CuN ₆ O ₂
Formula weight	343.42	748.36
Crystal size (mm ³)	0.64 × 0.13 × 0.07	0.40 × 0.26 × 0.10
Crystal color	orange	brown
Crystal system	orthorhombic	triclinic
Space group	<i>Pna</i> 2 ₁	<i>P</i> $\bar{1}$
Unit cell		
<i>a</i> (Å)	29.466(4)	12.0937(12)
<i>b</i> (Å)	10.1273(12)	14.1101(14)
<i>c</i> (Å)	6.1388(8)	14.2416(14)
α (°)	90	60.4500(10)
β (°)	90	65.7310(10)
γ (°)	90	64.9300(10)
<i>V</i> (Å ³)	1831.9(4)	1850.9(3)
<i>Z</i>	4	2
Absorption coefficient (mm ⁻¹)	0.08	0.637
Reflections collected	18061	21919
Independent reflections [<i>R</i> _{int}]	2491 [0.0394]	7585 [0.0360]
<i>R</i> ₁ , <i>wR</i> ₂ [<i>I</i> > 2σ(<i>I</i>)]	0.0414, 0.0965	0.0364, 0.0833
<i>R</i> ₁ , <i>wR</i> ₂ (all data)	0.0533, 0.1030	0.0517, 0.0902
CCDC number	841748	902594

refined using anisotropic atomic displacement parameters and hydrogen atoms bonded to carbon atoms were inserted at calculated positions using a riding model. The phenolic hydrogen atom in the ligand (*HL*) was located from difference maps and not further refined. Details of the crystal data and refinement are given in Table 1.

3. Results and discussion

3.1. Synthesis

The azo-azomethine ligand, 4-[(*E*)-phenyldiazenyl]-2-[(*E*)-{4-(propan-2-yl)phenyl}imino]methyl]phenol was prepared by reacting 4-isopropylaniline with 2-hydroxy-5-[(*E*)-phenyldiazenyl]

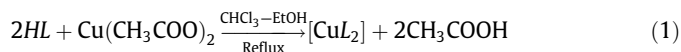


i: (1) NaNO₂, HCl, 0 °C, (2) salicylaldehyde; *ii*) 4-isopropylaniline, MeOH and reflux

Scheme 1. Preparation reaction of 4-[(*E*)-phenyldiazenyl]-2-[(*E*)-{4-(propan-2-yl)phenyl}imino]methyl]phenol, (*HL*) dye and its possible tautomeric equilibriums.

benzaldehyde obtained by treating a diazonium salt solution of aniline with salicylaldehyde in MeOH media with an aqueous solution of NaNO₂ at –5 °C. The general preparation scheme, involving aniline diazonium salt solution, diazo coupling and condensation, is shown in Scheme 1. The level of impurity in the product was checked by t.l.c. The synthesized ligand (*HL*) was subsequently characterized by its melting point, elemental analysis, FT-IR, ¹H and ¹³C NMR spectroscopic studies and CHN microanalysis. The results of these analyses are presented in experimental section and the mass, ¹H and ¹³C NMR spectra are displayed in Figs. 1–3, respectively. The elemental analysis results of the azo-azomethine ligand *HL* are in good agreement with the theoretical values.

The azo-azomethine ligand, 4-[(*E*)-phenyldiazenyl]-2-[(*E*)-{4-(propan-2-yl)phenyl}imino]methyl]phenol, formed a mononuclear complex with Cu(II) as following Eq. (1):



The structure of the Cu(II) complex was also elucidated using a number of analytical methods and spectroscopic techniques. The level of impurity in the product was also checked with t.l.c. The metal complex, [CuL₂], is stable in air as solid without decomposition, and soluble in chloroform, dichloromethane, dimethylsulfoxide and dimethylformamide and insoluble in *n*-hexane and water. Single crystals of the complex suitable for X-ray diffraction study were obtained from the CHCl₃ solution of the complex by slow evaporation.

The results of the elemental analyses of the compound are in good agreement with the theoretical values. The analyses of the [CuL₂] coordination compound indicate that the metal-ligand ratio is 1:2 in the Cu(II) complex.

3.2. ¹H- and ¹³C NMR spectra

The ¹H and ¹³C NMR spectral data of the bidentate azo-azomethine ligand recorded in CDCl₃ are given in experimental section. The NMR spectral analysis was carried out for the azo-azomethine

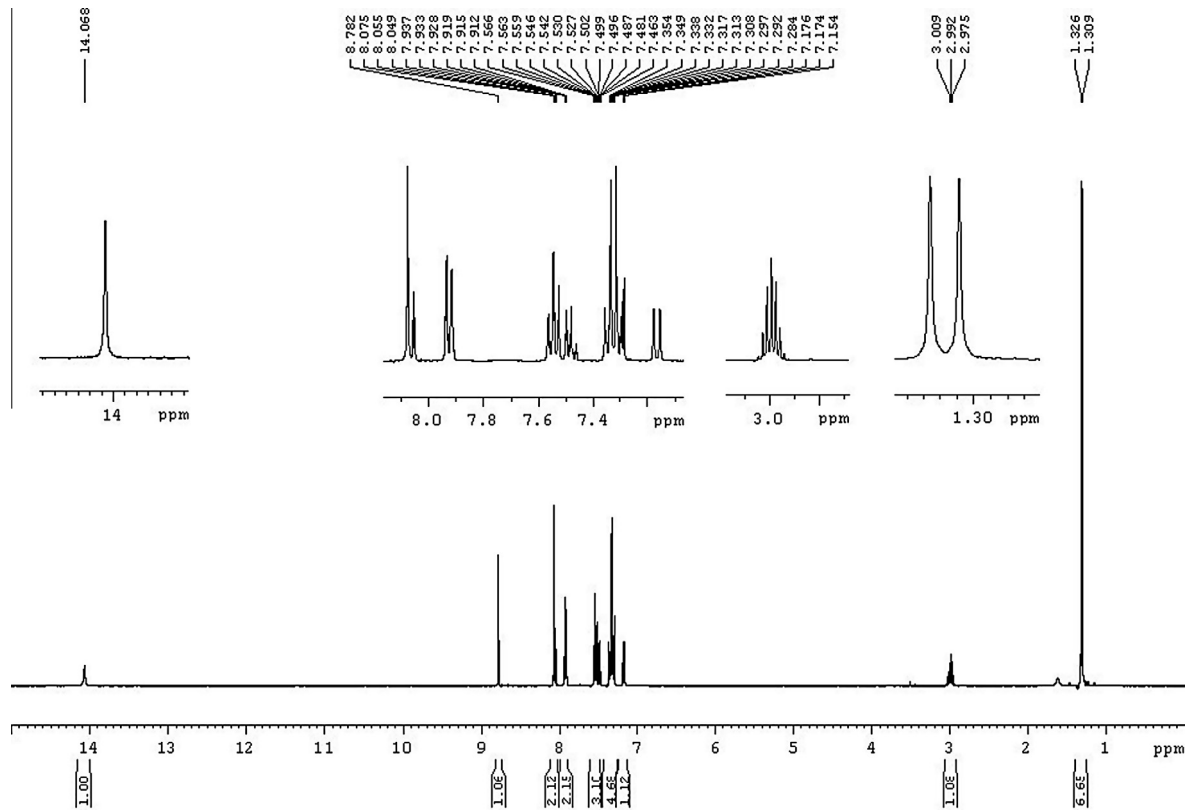


Fig. 1. ¹H NMR spectrum of the ligand HL.

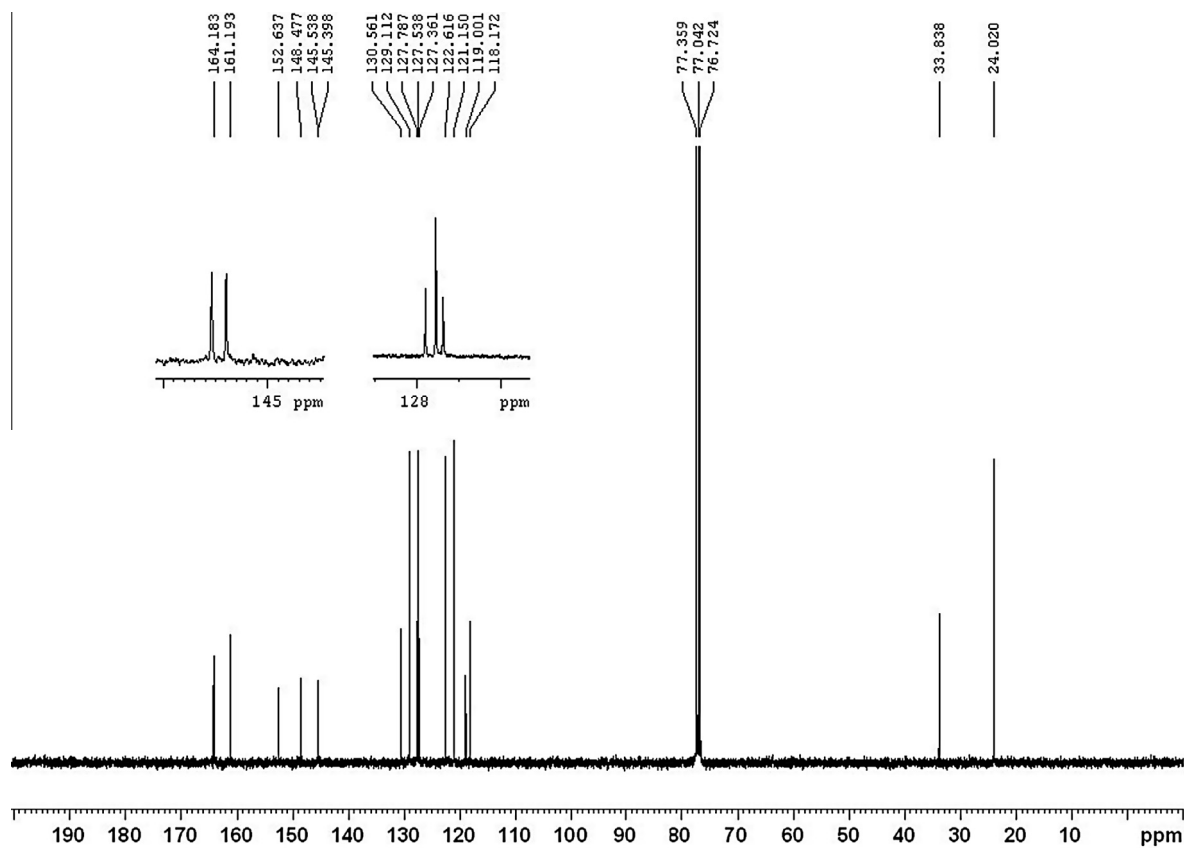


Fig. 2. ¹³C NMR spectrum of the ligand HL.

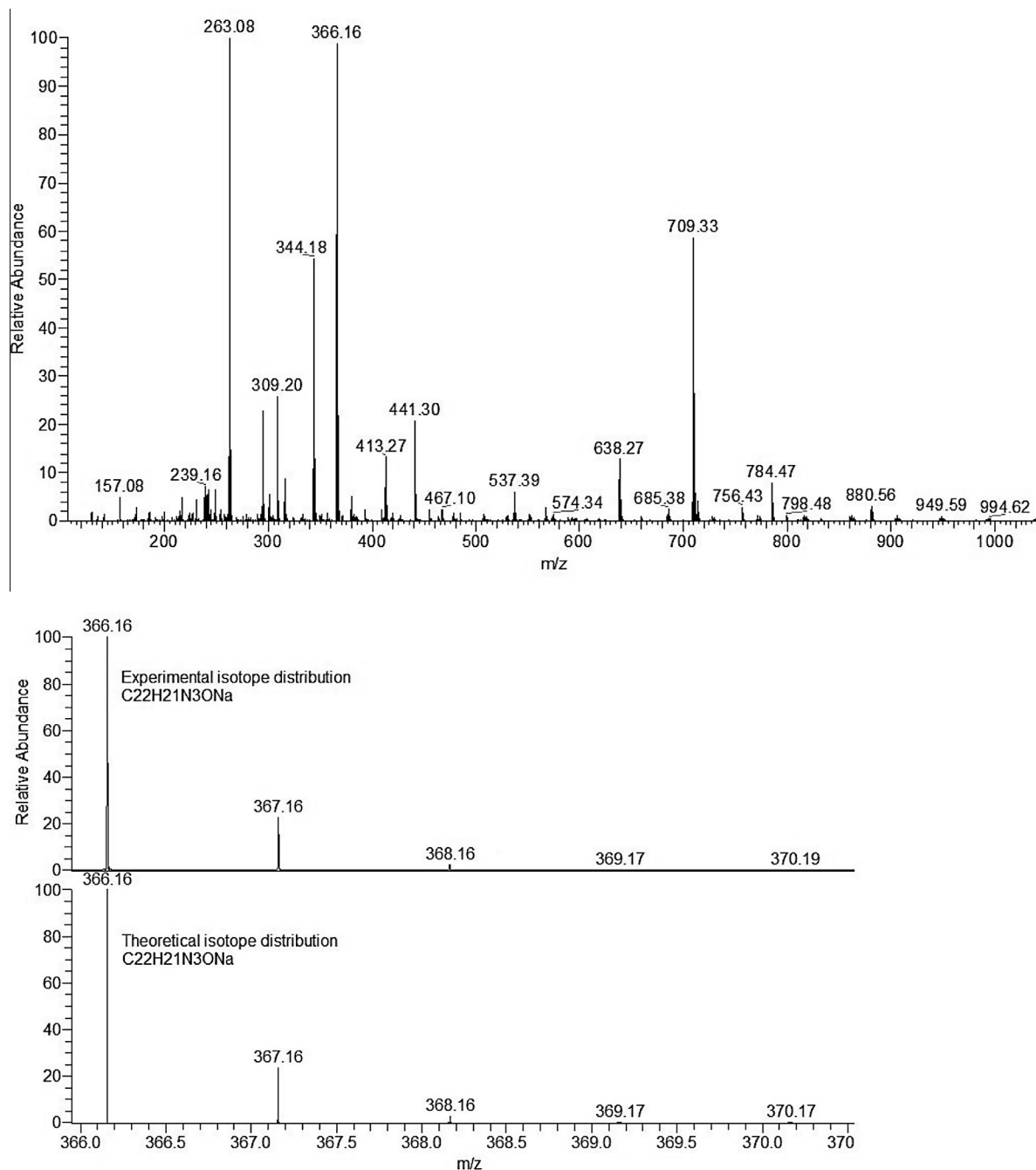


Fig. 3. Mass spectrum (top) and isotope distribution (bottom) of the ligand *HL*.

ligand synthesized which provided further evidence for the structural characteristics of the ligand. The spectra of *HL* ligand are shown in Figs. 1 and 2, respectively. The ¹H NMR spectrum of the ligand shows two peaks at 14.06 [44] and 8.78 ppm characteristic of the hydroxyl (O–H) and azomethine (–CH=N–) protons, respectively [40]. This indicates that the azo-imine form is more stable than other forms in CDCl₃. The signals associated with different aromatic and aliphatic protons can be observed in the spectrum. The peaks at 7.17 (d, CH¹³, *J* = 8.27 Hz), 7.31 (d, CH¹⁴, *J* = 6.13 Hz), 7.33 (d, CH^{5,9}, *J* = 7.66 Hz), 7.35 (s, CH¹⁶), 7.49 (t, CH²⁰, *J* = 6.76 Hz), 7.56 (t, CH^{19,21}, *J* = 7.37 Hz), 8.04 (d, CH^{6,8}, *J* = 8.45 Hz), and 8.07 ppm (d, CH^{18,22}, *J* = 9.78 Hz) were assigned to the aromatic protons. As expected, the isopropyl group showed two signals at 1.32 (d, CH₃^{1,2}, *J* = 6.92 Hz) and 2.99 (st, CH³,

J = 6.93 Hz) are due to CH₃^{1,2} and methylene CH³ protons according to the chemical shift.

The ¹³C NMR spectrum of the ligand exhibited the signals due to the presence of aromatic and aliphatic carbons. The presence of azomethine group is evident from the characteristic signal at the farthest downfield (~164.23 ppm) corresponding to the carbon of azomethine group (C¹⁰). The peak at 164.18 ppm was assigned to the aromatic carbon linked hydroxyl group (C¹²). The aliphatic region of the ¹³C NMR spectrum of *HL* showed two peaks as seen in Fig. 2. The medium intense peak CH₃ (24.02 ppm, C¹, C²) was conveniently assigned to the methyl carbon of the isopropyl group. The peak –CH– (33.83 ppm, C³) is due to tertiary carbon according to the chemical shift. In the aromatic region of the ¹³C NMR spectrum of compound *HL*, the peaks at 119.00 (C¹¹), 121.15 (C⁶, C⁸),

122.61 (C¹⁶), 127.36 (C¹⁴), 127.53 (C⁵, C⁹), 127.78 (C¹⁹, C²¹), 130.56 (C²⁰), 145.53 (C¹⁵), 148.47 (C⁴), 152.63 (C⁷) and 161.19 (C¹⁷) ppm were assigned to the aromatic carbons. The peaks were then tentatively assigned by matching the observed and calculated chemical shifts. The spectroscopic data obtained in this work are agreed well with previous works [40].

3.3. FT-IR spectra

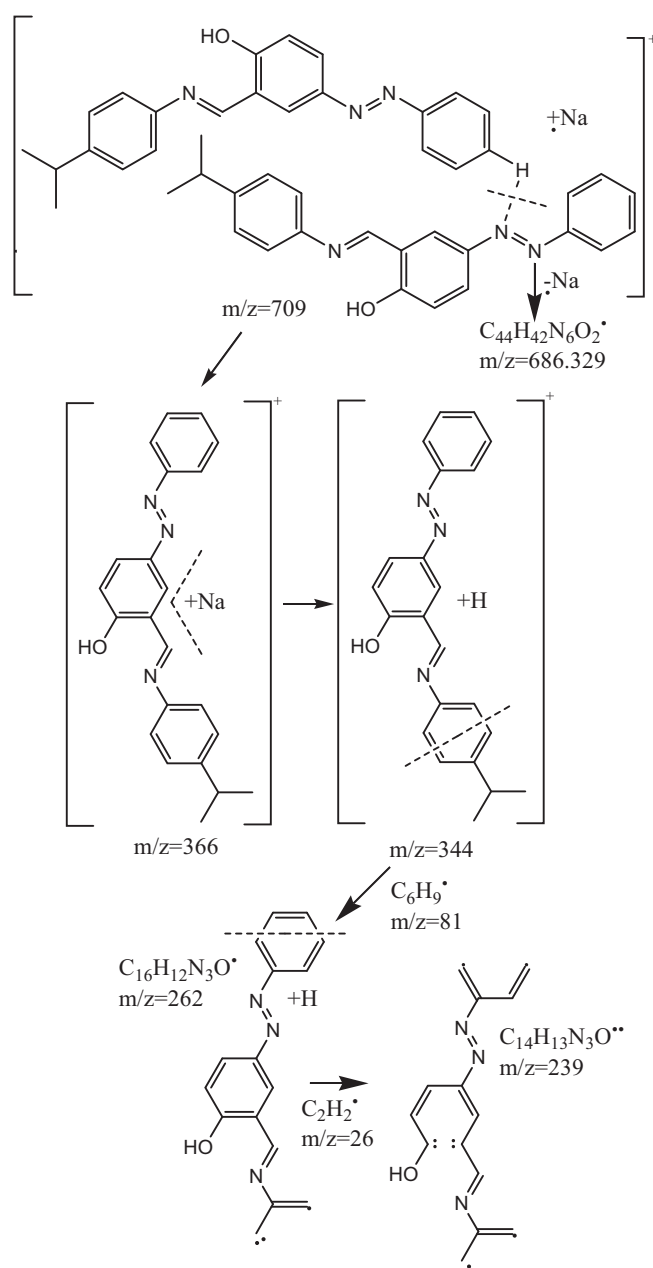
The important infrared characteristic absorption bands of the ligand and its copper(II) complex, along with their proposed assignments, are summarized in experimental section. The functional groups of the azo-azomethine ligand and its copper(II) chelate have been identified from their infrared spectra. Schiff bases are capable of forming coordinate bonds with many metal ions through both azomethine group and phenolic group or *via* its azomethine or phenolic groups. A strong absorption band at

3320 cm⁻¹ and comparatively weak band at 1616 cm⁻¹ were assigned to phenolic OH [45] and azomethine C=N stretching vibrations of the azomethine ligand containing -N=N- chromophore, respectively [46,47]. The absence of band due to phenolic OH group in the spectrum of the metal complex suggests the coordination of ligand to the metal *via* deprotonation. A strong band observed in the IR spectrum of the ligand in the region of 3400–3200 cm⁻¹ is due to hydrogen bonded ν(OH) in the azo tautomer. In the copper(II) complex, the band at 1616 cm⁻¹ shifted toward lower frequency because of the coordination of the nitrogen to the copper ion. This fact can be explained by the withdrawing of electrons from nitrogen atom to the metal ion due to coordination. The aromatic and aliphatic (isopropyl) moieties in the ligand can be identified by the bands at 3050 cm⁻¹ (aromatic C-H stretching) and 2957 cm⁻¹ (aliphatic C-H stretching). The ligand exhibits a broad medium intensity band at 2700 cm⁻¹, which is assigned to the intramolecular hydrogen-bonding O-H...N vibration. This situation is common for aromatic azomethine compounds containing *o*-OH groups, and in the complex this band disappears completely.

The complex [CuL₂] shows a band at 1471 cm⁻¹ could be assigned to the -N=N- azo group. The new band at 589 cm⁻¹ for the Cu(II) complex is assigned to (Cu-O) [48]. The band observed at 462 cm⁻¹ can be assigned to (Cu-N), indicating the participation of azomethine nitrogen in the coordination to copper ion. Accordingly, the azo-azomethine ligand acts as monobasic bidentate chelating agent coordinated to copper(II) *via* the azomethine-nitrogen and phenol-oxygen atoms forming the more stable six-membered chelate ring. A medium intensity band in the region 2921–2956 cm⁻¹ is due to the aliphatic (C-H) stretching. The weak absorption peak observed at 3065 cm⁻¹ is attributed to the (C-H) of the phenyl rings. A comparison between infrared spectra of *HL* and the [CuL₂] complex also show that a band, characteristic of ν(C-O) at 1315 cm⁻¹, shifted to 1345–1325 cm⁻¹, due to C-O-Cu bond formation.

3.4. Mass spectra

The mass spectral studies the azo-azomethine ligand (*HL*) and its metal complex [CuL₂] were performed using ESI method and obtained data are given in experimental section. The mass spectrum and isotope distribution of the ligand (*HL*) is shown in



Scheme 2. Mass fragmentation pattern of the azo-azomethine dye (*HL*).

Table 2
UV-Visible absorption spectra of *HL* and [CuL₂] in various solvents.

Compounds	Solvent	λ_{max} (nm, L mol ⁻¹ cm ⁻¹ × 10 ³)
<i>HL</i>	Dichloromethane	235 (30.43), 335 (10.20)
	Chloroform	230 (30.88), 335 (10.02)
	Dimethylformamide	240 (30.27), 330 (10.89)
	Dimethylsulfoxide	235 (33.43), 335 (7.30)
[CuL ₂]	Dichloromethane	230 (34.12), 305 (11.92), 385 (21.09)
	Chloroform	235(30.56), 300 (10.90), 385(19.52)
	Dimethylformamide	245(30.88), 295 (16.32), 375(20.09)
	Dimethylsulfoxide	240(33.48), 301 (7.20), 390 (10.98)

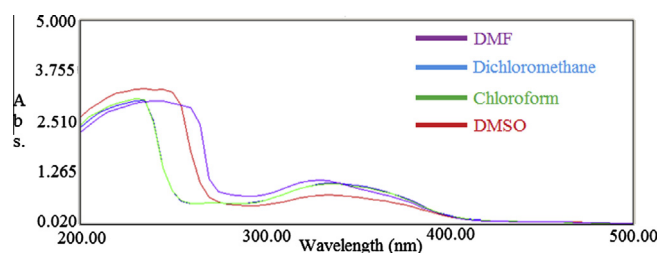


Fig. 4. Absorption spectra of the azo-azomethine dye in various solvents.

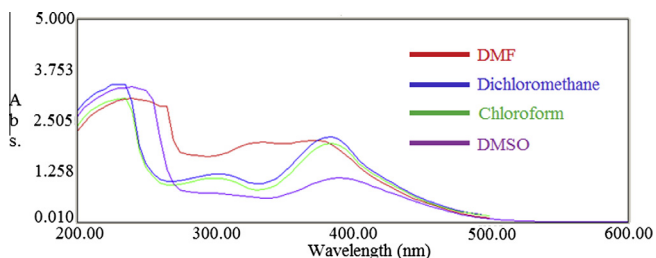


Fig. 5. Absorption spectra of the Cu(II) complex in various solvents.

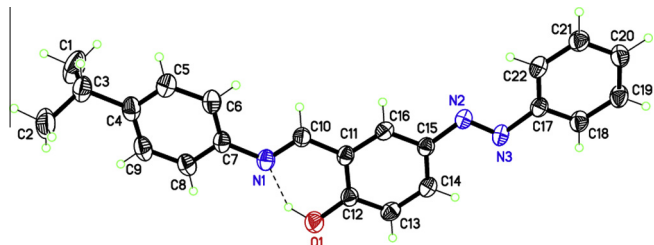


Fig. 6. Perspective view of the ligand HL with atom numbering; thermal ellipsoid 50% probability, the hydrogen bond is shown as a dashed line.

Table 3
Selected bond lengths and angles [Å and °] for the ligand (HL).

N(1)–C(10)	1.280(3)	C(10)–N(1)–C(7)	122.1(2)
C(7)–N(1)	1.421(3)	O(1)–C(12)–C(13)	118.79(19)
C(12)–O(1)	1.346(2)	O(1)–C(12)–C(11)	121.16(19)
C(15)–N(2)	1.420(3)	C(14)–C(15)–N(2)	124.98(18)
N(2)–N(3)	1.259(2)	C(16)–C(15)–N(2)	115.92(19)
N(3)–C(17)	1.434(3)	C(22)–C(17)–N(3)	123.94(18)
		N(2)–N(3)–C(17)	113.57(17)
C(8)–C(7)–N(1)	116.7(2)	C(18)–C(17)–N(3)	115.89(18)
C(6)–C(7)–N(1)	124.7(2)	N(3)–N(2)–C(15)	114.45(17)
N(1)–C(10)–C(11)	121.4(2)		

Fig. 3 and the fragmentation pattern for the ligand is presented in Scheme 2. The mass spectrum of the azo-azomethine ligand showed signals at m/z 344 (40%) and 366 (100%) assigned to $[M+1]^+$ and $[M+Na]^+$, respectively. The experimental isotope

Table 4
Hydrogen-bond geometry (Å, °) for the ligand (HL).

D–H...A	D–H	H...A	D...A	D–H...A
C20–H20...N2 ⁱ	0.95	2.83	3.509 (3)	129.6
C10–H10...O1 ⁱⁱ	0.95	2.82	3.585 (3)	138.6
C13–H13...C8 ⁱⁱⁱ	0.95	2.85	3.606 (3)	137.0
C13–H13...C7 ⁱⁱⁱ	0.95	2.84	3.359 (3)	115.6
O1–H1...N1	0.94	1.75	2.580 (3)	145.3

Symmetry codes: (i) $-x+1/2, y-1/2, z+1/2$; (ii) $x, y, z+1$; (iii) $-x+1, -y+2, z-1/2$.

distribution for $[M+1]^+$ is well agreed with the theoretical isotope distribution (Fig. 3). The mass spectrum of the ligand shows two fragmentation peaks at m/z 262 and m/z 239. These peaks can be attributed to the $[C_{16}H_{12}N_3O+1]^+$ and $[C_{14}H_{13}N_3O]^+$ ions, respectively. On the other hand, a peak at m/z 686 can be assigned to $[2M]^+$ dimeric structure ion. The higher mass peak at m/z 709 (60%) can be attributed to $[2M+Na]^+$. The mass spectrum of the copper(II) complex shows molecular ion signal at m/z 770 assigned to $[M+Na-1]^+$. Moreover, the fragmentation peaks at m/z 537 and m/z 468 can be attributed to the $[C_{32}H_{31}CuN_2O_2-1]^+$ and $[C_{27}H_{21}CuN_2O_2-1]^+$ ions, respectively.

3.5. Electronic spectra

The UV–Visible spectra of the HL azo-azomethine ligand and its copper(II) metal chelate, $[CuL_2]$ in various solvents with different polarities such as chloroform, dichloromethane, dimethylformamide and dimethylsulfoxide between 200 and 800 nm were taken and their wave lengths of absorption maximum are reported in Table 2. The spectra of the HL and $[CuL_2]$ compounds in various solutions are shown in Figs. 4 and 5, respectively. The spectroscopic data obtained in this work are agreed well with the previous work [40]. Electronic spectrum of the HL ligand in these solvents showed broad absorption bands in the range of 230–240 nm. These absorption bands can be attributed to $\pi \rightarrow \pi^*$ transitions [40,41]. The $\pi \rightarrow \pi^*$ transitions are low energy transitions observed in organic molecules and are used in structural analysis. Since the azo-azomethine ligand contains an imine ($-HC=N-$) and an azo ($-N=N-$) chromophore groups, the $\pi \rightarrow \pi^*$ transition of the ligand observed in different wavelengths in different solvents, which can be attributed to the polarity of the used solvent. In general, the

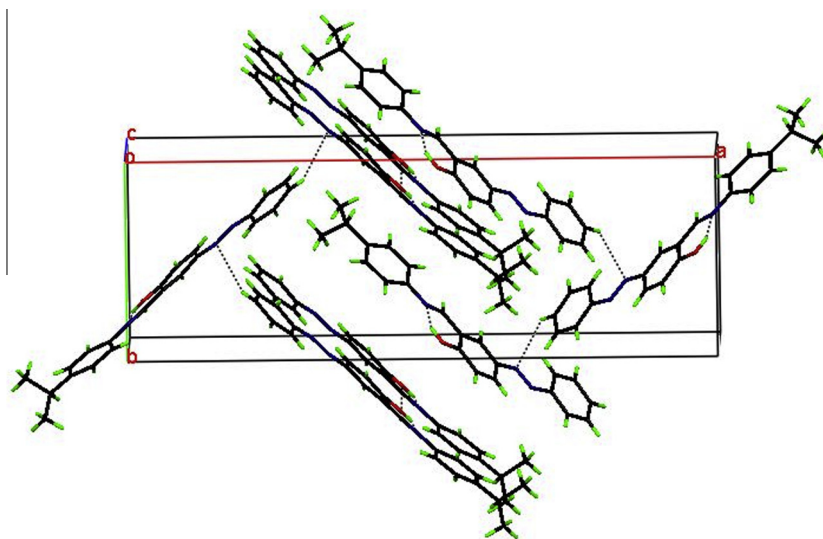


Fig. 7. Packing plot of the ligand HL viewing down c axis, hydrogen bonds are shown as dashed lines.

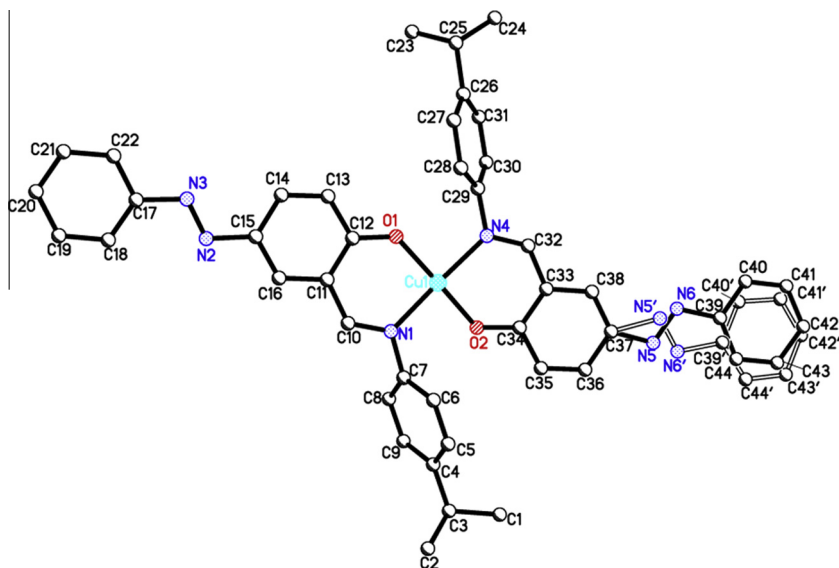


Fig. 8. Perspective view of the complex $[\text{CuL}_2]$.

Table 5

Selected bond lengths and angles [Å and °] for the complex $[\text{CuL}_2]$.

Cu(1)–O(1)	1.8701(13)	Cu(1)–N(1)	2.0102(16)
Cu(1)–O(2)	1.8787(14)	Cu(1)–N(4)	2.0175(16)
O(1)–Cu(1)–O(2)	172.24(6)	O(1)–Cu(1)–N(4)	88.84(6)
O(1)–Cu(1)–N(1)	92.23(6)	O(2)–Cu(1)–N(4)	91.98(6)
O(2)–Cu(1)–N(1)	87.66(6)	N(1)–Cu(1)–N(4)	174.65(6)

$\pi \rightarrow \pi^*$ transitions shift to longer wavelengths as the polarity of the solvent increases. Due to the dipole moment of the solvent, a new dipole moment on the ligand is formed. This solvent effect is greater on the π^* orbital than the π orbital. Therefore, the energy of the $\pi \rightarrow \pi^*$ transitions decreases as the energy level of the π^* orbital decreases and, the $\pi \rightarrow \pi^*$ transition absorption red shifts. However, in the UV–Visible spectrum of the ligand, weaker and broader (compare to the $\pi \rightarrow \pi^*$ transitions) absorption bands in the range of 300–400 nm were observed. These transition bands could be attributed to the $n \rightarrow \pi^*$ transitions due to the presence of n electrons on the $-\text{CH}=\text{N}-$ or $-\text{N}=\text{N}-$ chromophore groups. Thus, the $n \rightarrow \pi^*$ transition bands shifted to shorter wavelengths in more polar solvents. Similar absorption bands were observed for the $[\text{CuL}_2]$ metal chelate in the same region. An additional band was observed at around 375–390 nm assigned to the coordination of azomethine nitrogen atom to the metal center. These bands were assigned to both a charge transfer transition from the metal

to antibonding orbital of the ligand and a spin-allowed transition of the ligand. However, no absorption band attributed to the d–d transitions in the metal center was observed. It may be lost in the low-energy tail of the intense transition.

3.6. Crystal structure of the azo-azomethine ligand (HL)

The ligand can be easily isolated as crystalline material with a sharp melting point therefore its molecular structure can also be characterized by single crystal X-ray analysis, the most straightforward technique to confirm the identity. The title compound crystallizes in the non-centric *orthorhombic* space group $Pna2_1$. A perspective view of the molecule with atom numbering is shown in Fig. 6. Selected bond lengths and angles are given in Table 3, all bond lengths and angles are within the normal ranges. The diazenyl ($-\text{N}_2=\text{N}_3$) and azomethine ($-\text{C}_{10}=\text{N}_1-$) linkages are 1.259(2) and 1.280(3) Å, respectively; similar to those observed for related azo-azomethine compounds [29,30]. In the structure, both outer rings slightly twisted with respect to the central benzene ring. The mean planes of C4–C9 and C17–C22 are at 10.30(14) and 12.23(12)° to the central (C11–C16) ring, respectively. Aromatic rings (C4–C9) and (C11–C16) adopt the *trans* configuration with regard to the azo double bond ($-\text{N}=\text{N}-$) with the torsion angle C(15)–N(2)–N(3)–C(17) of 178.18(17)° which is in good agreement with published values [29]. There is an intramolecular phenol-imine hydrogen bond

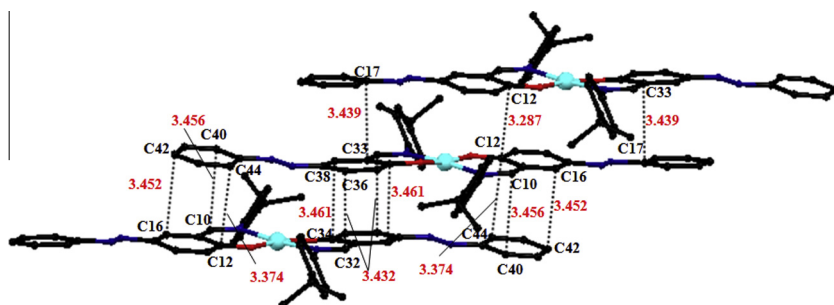
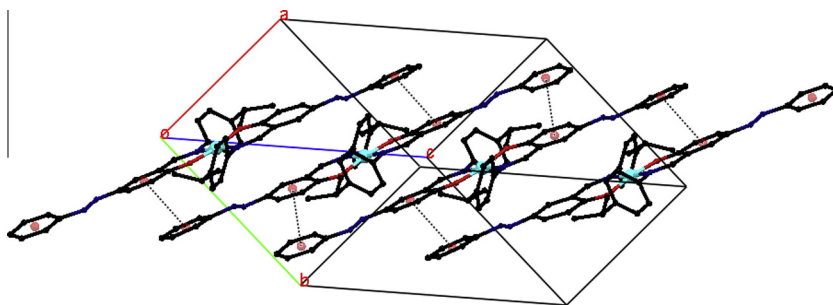
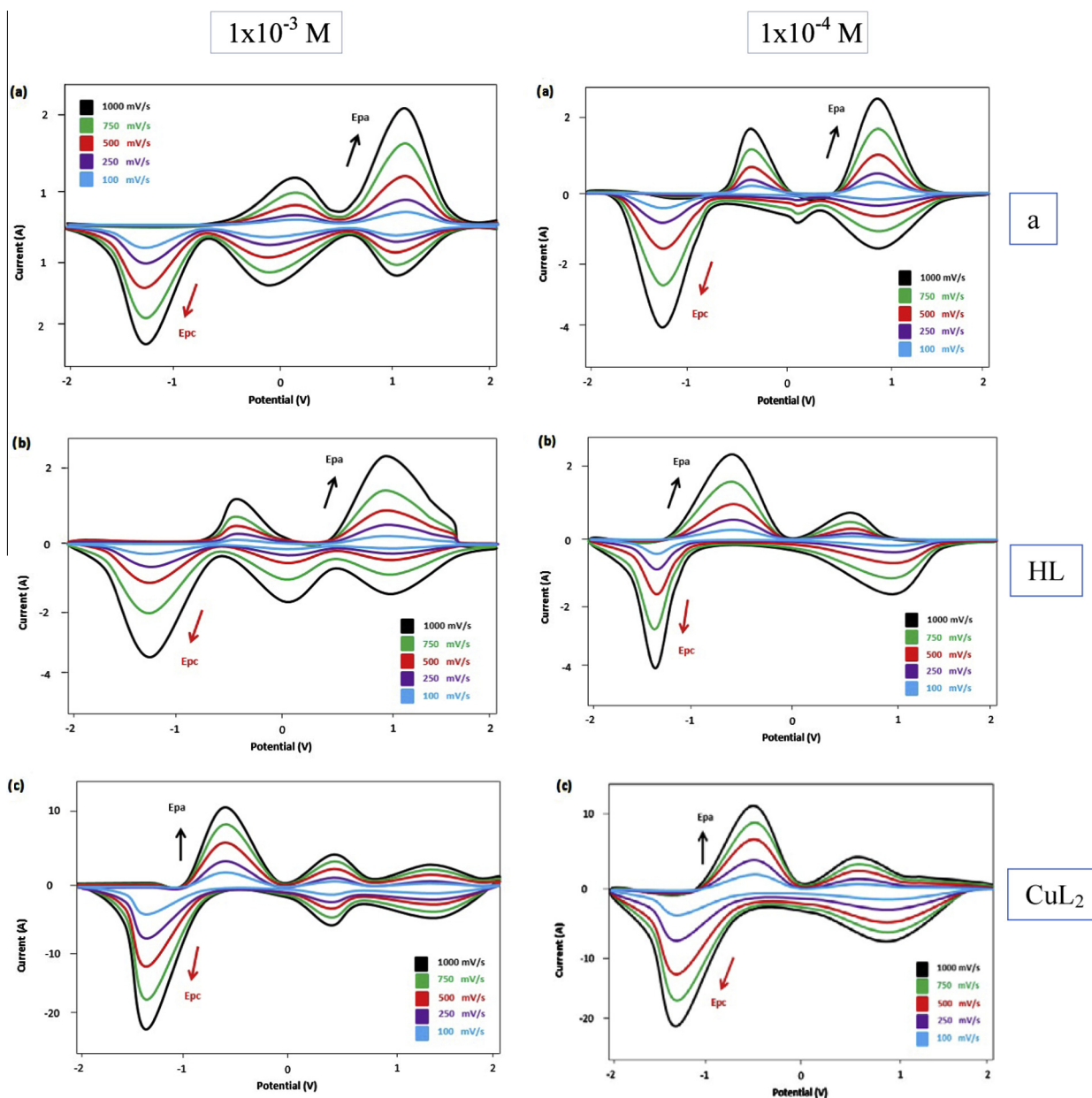


Fig. 9. π – π stacking interactions in $[\text{CuL}_2]$.

Fig. 10. Packing diagram of $[\text{CuL}_2]$.Fig. 11. Cyclic voltammograms of the synthesized compounds in the presence of 0.1 M NBu_4BF_4 -DMF solution.

(O1...N1) with a distance of 2.580(3) Å forming a S(6) hydrogen bonding motif. There are also weak intermolecular hydrogen bond type interactions C10–H...O and C20–H...N(2)=N(3) (with D...A distances of 3.585(3) and 3.509(3) Å, respectively) stabilizing the structure (Fig. 7). Hydrogen bond parameters are listed in Table 4.

3.7. Crystal structure of the complex [CuL₂]

The structure was solved in the *triclinic* space group $P\bar{1}$. The molecular structure is depicted in Fig. 8. Selected bond lengths and angles are listed in Table 5. All bond lengths and angles are within the normal ranges. The asymmetric unit contains two independent bi-dentate azo-azomethine ligands and one Cu(II) center. Azo-benzene moiety (N5–C44) of the one of the ligands is disordered and this was modelled over two positions with 60:40 occupancy (N5–C44; N5'–C44'). The Cu(II) ion is coordinated to two phenolate oxygen atoms and two imine nitrogen atoms of two azo-azomethine molecules with approximate square planar geometry. The Cu–O bonds are in *trans* configuration and Cu–O distances are shorter than Cu–N distances.

The *iso*-propylbenzene ring in both independent ligands significantly twisted with respect to the central phenolate ring with the dihedral angles of 66.93(7)° for rings C4–C9 and C11–C16 and 64.59(6)° for C26–C31 and C33–C38 this is probably due to minimize the steric hindrance to bind metal center.

The principal interactions between complex molecules are π – π stacking interactions. There are two sets of the structure illustrated in Fig. 9. Crystal packing of the complex molecules is determined by π – π stacking interactions. Packing diagram is shown in Fig. 10.

3.8. Thermal analysis

Thermogravimetric analysis of the azo-azomethine ligand *HL* and its Cu(II) complex were examined under N₂ atmosphere and the TG/DTA curves are shown in Figs. S1 and S2. The ligand *HL* shows a weight loss of $\approx 0.4\%$ in the temperature range 103–183 °C accompanied by an endothermic peak with $T_{\max} = 145$ °C on the DTA curve. The loss may be due to small amount of moisture in the sample. The main framework of the ligand is thermally stable up to 183 °C. The $\approx 54\%$ of the sample decomposes in the temperature range 183–404 °C with an exothermic peak ($T_{\max} = 331$ °C). The rest of the organic moiety gradually decomposes up to higher temperatures.

Thermogravimetric data shows that the Cu(II) complex thermally more stable than the azo-azomethine compound (*HL*). The Cu(II) complex [CuL₂] exhibits a weight loss of $\approx 1.3\%$ in the temperature range 103–183 °C and this weight loss was attributed to small amount of moisture in the sample. The loss in the temperature range 103–183 °C follow an endothermic peak with $T_{\max} = 190$ °C. The $\approx 47.6\%$ of the sample decomposed in the temperature range 226–458 °C with an endothermic (274 °C) and an exothermic (330 °C) peaks. Rest of the organic moiety slowly decomposes up to higher temperatures (up to 1000 °C) leaving CuO as final residue.

3.9. Electrochemistry

Electrochemical properties of the synthesized azo-aldehyde (a), azo-azomethine (*HL*) and its Cu(II) complex [CuL₂] were studied in DMF – 0.1 M NBu₄BF₄ as supporting electrolyte at room temperature. Electrochemical behaviors of the compounds were investigated in two different concentrations (1×10^{-3} and 1×10^{-4} M) and five different scan rates (in the 100–1000 mV/s range) against

Table 6
The electrochemical data of the synthesized compounds.

Compounds	Conc. (M)	Scan-rate (mV/s)	E_{pa} (V)	E_{pc} (V)	$E_{1/2}$ (V)	I_{pa}/I_{pc}	ΔE_p (V)	
(a)	1×10^{-3}	100	–0.30, 0.94	0.94, 0.09, –1.13	0.94	1.00	0.83	
		250	–0.33, 0.86	0.86, 0.12, 1.17	0.86	1.00	0.84	
		500	–0.40, 0.85	0.85, 0.15, –1.23	0.85	1.00	0.83	
		750	–0.45, 0.80	0.80, 0.21, –1.26	0.80	1.00	0.81	
		1000	–0.54, 0.77	0.77, 0.24, –1.33	0.77	1.00	0.79	
	1×10^{-4}	100	–0.50, 0.63	1.00, –1.13	–	0.63	0.63	
		250	–0.53, 0.56	0.95, –1.20	–	0.58	0.67	
		500	–0.56, 0.53	0.93, –1.23	–	0.43	0.67	
		750	–0.60, 0.46	0.90, –1.30	–	0.51	0.70	
		1000	–0.66, 0.40	0.87, –1.33	–	0.45	0.67	
	<i>HL</i>	1×10^{-3}	100	–0.67, 0.30, 1.33	1.33, 0.30, –1.30	0.30	1.00	0.63
			250	–0.64, 0.33, 1.36	1.36, 0.33, –1.33	0.33	1.00	0.69
			500	–0.61, 0.39, 1.43	1.43, 0.39, –1.35	0.39	1.00	0.74
			750	–0.54, 0.42, 1.47	1.47, 0.42, –1.43	0.42	1.00	0.89
			1000	–0.45, 0.48, 1.50	1.50, 0.48, –1.49	0.48	1.00	1.04
1×10^{-4}		100	–0.46, 0.34	0.79, –1.30	–	0.37	0.84	
		250	–0.43, 0.37	0.81, –1.33	–	0.41	0.90	
		500	–0.40, 0.40	0.84, –1.40	–	0.47	1.00	
		750	–0.38, 0.42	0.87, –1.43	–	0.48	1.05	
		1000	–0.34, 0.45	0.90, –1.47	–	0.50	1.13	
[CuL ₂]		1×10^{-3}	100	0.09, 1.06	1.06, –0.06, –1.33	1.06	1.00	0.15
			250	0.10, 1.12	1.12, –0.09, –1.30	1.12	1.00	0.19
			500	0.12, 1.21	1.21, –0.12, –1.23	1.21	1.00	0.24
			750	0.14, 1.27	1.27, –0.15, –1.16	1.27	1.00	0.29
			1000	0.15, 1.33	1.33, –0.21, –1.13	1.33	1.00	0.36
	1×10^{-4}	100	–0.45, 0.85	0.85, –1.16	0.85	1.00	0.71	
		250	–0.42, 0.80	0.80, –1.20	0.80	1.00	0.78	
		500	–0.36, 0.74	0.74, –1.26	0.74	1.00	0.90	
		750	–0.30, 0.71	0.71, –1.30	0.71	1.00	1.00	
		1000	–0.27, 0.65	0.65, –1.36	0.65	1.00	1.09	

* E_{pa} and E_{pc} are anodic and cathodic potentials, respectively. $E_{1/2} = 0.5 \times (E_{pa} + E_{pc})$, $\Delta E_p = E_{pa} - E_{pc}$.

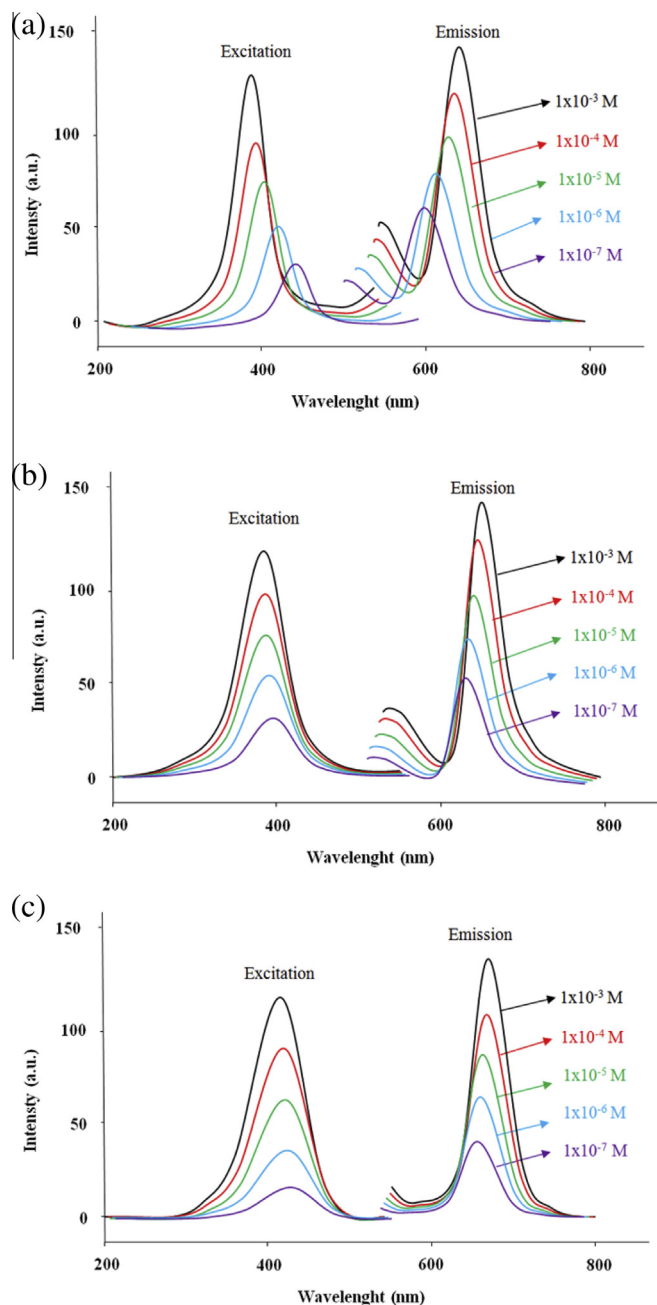


Fig. 12. The fluorescence emission and excitation spectra of the compound (a) azo-aldehyde (a), (b) *HL*, (c) $[CuL_2]$ in various concentrations (1.0×10^{-3} to 1.0×10^{-7} M, DMF).

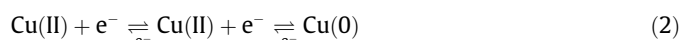
ferrocene–ferrocenium standard. The electrochemical curves of synthesized compounds are shown in Fig. 11. The data are given in Table 6. The azo-aldehyde in the 1×10^{-3} M shows two reversible anodic peak potentials (0.09 and 1.33 V) in 100–1000 mv/s scan rate range and three cathodic peak potentials in the -1.33 to 1.17 V range. In the 1×10^{-4} M and scan rates range studied, the azo-aldehyde (a), there are two anodic and cathodic peak potentials are observed. The oxidation and reduction processes of the compound in this concentration (1×10^{-4} M) are irreversible. The azo ($-N=N-$) chromophore group containing Schiff base ligand (*HL*) in the 1×10^{-3} M and 100–1000 mv/s range shows the two reversible anodic peak potentials in the -0.54 to 0.94 V range. In this scan rate range, the ligand shows three cathodic peak potentials in the -1.33 to 0.94 V range. However, one of the cathodic

Table 7

The photoluminescence data for the prepared compounds.

Compounds	Conc.(M)	Excitation		Emission	
		λ (nm)	Intensity (a.u)	λ (nm)	Intensity (a.u)
(a)	1×10^{-3}	385	134	629	144
	1×10^{-4}	387	98	624	138
	1×10^{-5}	392	78	618	97
	1×10^{-6}	416	45	602	74
	1×10^{-7}	439	32	595	69
<i>HL</i>	1×10^{-3}	394	124	625	140
	1×10^{-4}	396	96	621	128
	1×10^{-5}	398	72	618	92
	1×10^{-6}	400	53	615	65
	1×10^{-7}	402	38	611	51
$[CuL_2]$	1×10^{-3}	408	127	678	130
	1×10^{-4}	410	87	670	109
	1×10^{-5}	412	62	664	84
	1×10^{-6}	414	36	658	68
	1×10^{-7}	420	18	650	36

peak potentials observed in 1×10^{-3} M disappeared and all reduction and oxidation processes are irreversible in 1×10^{-4} M concentration. The cyclic voltammograms for the Cu(II) complex in the 100–1000 mv/s range exhibits three anodic and three peak potentials in 1×10^{-3} M. However, in 1×10^{-4} M, there are two anodic and two cathodic peak potentials. All the oxidation and reduction processes of the complex at both concentrations are reversible. As the scan rate increases, the cathodic and anodic peak potentials shifted to more negative or positive regions. In the reversible electrochemical processes of the Cu(II) complex may be proposed as shown Eq. (2).



3.10. Photoluminescence

The effect of different concentration on the photoluminescence properties of the azo-aldehyde (a), azo-azomethine ligand *HL* and its Cu (II) complex $[CuL_2]$ was investigated in the 1.0×10^{-3} to 1.0×10^{-7} M range in DMF solution. The emission and excitation spectra of the synthesized compounds containing an azo chromophore group ($-N=N-$) are shown in Fig. 12a–c and the data are given in Table 7. The azo-aldehyde (a) and the azo-azomethine ligand *HL* exhibit only one emission maxima in the 595–629 nm range upon excitation in the 385–439 nm range. Both emission and excitation intensities increased with the increase in concentration. When concentration increased emission maxima for the azo-aldehyde (a) and ligand (*HL*) shifted to higher wavelength values (lower energy regions).

The complex $[CuL_2]$ exhibits similar excitation and emission spectra to the azo-azomethine ligand (Fig. 12c). However, upon coordination with Cu(II) ion, both excitation and emission intensities shifted to lower values. The reason why both excitation and emission intensities reduced can be due to complex formation with the Cu(II) ion. Therefore, the energy transfer from the excited state of the ligand (*HL*) to the Cu(II) ion might be possible, hence non-radiated transition of the ligand excited state increases and declines the emission intensity [49].

4. Conclusion

In summary, azo-azomethine ligand 4-[(*E*)-phenyldiazenyl]-2-[(*E*)-{[4-(propan-2-yl)phenyl]imino}methyl]phenol (*HL*) derived from 2-hydroxy-5-[(*E*)-phenyldiazenyl]benzaldehyde (a) was synthesized and characterized. Elemental analyses confirms the

chemical composition of the synthesized compounds while FT-IR, mass, ^1H - and ^{13}C NMR spectroscopy confirms the functional groups, particularly $-\text{N}=\text{N}-$ and $-\text{HC}=\text{N}$ imine groups, of the ligand. The metal-to-ligand ratio of the copper(II) complex was found to be 1:2 and, thus, the copper(II) ion appears to be four coordinated with the *O*; *N*-monobasic bidentate ligand. Molecular structures of the ligand and its copper(II) chelate were successfully determined by single-crystal X-ray diffraction. The thermal data showed that the complex $[\text{CuL}_2]$ is thermally more stable than the ligand (*HL*) and the complex started to decompose at 226 °C. Electronic spectrum of the *HL* ligand exhibit two absorption bands in the range of 230–240 and 300–400 nm assigned to $\pi \rightarrow \pi^*$ and $n \rightarrow \pi^*$ transitions, respectively. Electrochemical and photoluminescence properties of the synthesised compounds were investigated.

Acknowledgments

The authors thank Research Found of Kahramanmaraş Sutcu Imam University for financial support (Project No: 2011/8-5 YLS), Kahramanmaraş, Turkey. The authors are grateful to the Department of Chemistry, Loughborough University, Leicester, UK for providing laboratory and analytical facilities.

Appendix A. Supplementary material

CCDC 841748 and 902594 contains the supplementary crystallographic data for the ligand and its Cu(II) complex. These data can be obtained free of charge from The Cambridge Crystallographic Data Centre via www.ccdc.cam.ac.uk/data_request/cif. Supplementary data associated with this article can be found, in the online version, at <http://dx.doi.org/10.1016/j.ica.2015.03.010>.

References

- [1] R. Gup, E. Giziroglu, B. Kirkan, *Dyes Pigments* 73 (2007) 40.
- [2] H.E. Katz, K.D. Singer, J.E. Sohn, C.W. Dirk, L.A. King, H.M. Gordon, *J. Am. Chem. Soc.* 109 (1987) 6561.
- [3] T. Abe, S. Mano, Y. Yamada, A. Tomotake, *J. Imag. Sci. Technol.* 43 (1999) 339.
- [4] S. Wang, S. Shen, H. Xu, *Dyes Pigments* 44 (2000) 195.
- [5] K. Maho, T. Shintaro, K. Yutaka, W. Kazuo, N. Toshiyuki, T. Mosahiko, *Jpn. J. Appl. Phys.* 42 (2003) 1068.
- [6] D.W. Rangnekar, V.R. Kanetkar, J.V. Malanker, G.S. Shankarling, *Indian J. Fibre Text. Res.* 24 (1999) 142.
- [7] P. Gregory, D.R. Waring, G. Hallos (Eds.), *The Chemistry and Application of Dyes*, Plenum Press, London, 1990, p. 18.
- [8] S.S. Kondil, *Transition Met. Chem.* 23 (1998) 461.
- [9] J.W. Daniel, *Toxicol. Appl. Pharmacol.* 4 (1962) 572.
- [10] J.A.C. Broekaert, *Anal. Chim. Acta* 124 (1981) 421.
- [11] M. Kurtoglu, N. Birbicer, U. Kimyonsen, S. Serin, *Dyes Pigments* 41 (1999) 143.
- [12] A.A. Jarrahpour, M. Motamedifar, K. Pakshir, N. Hadi, M. Zarei, *Molecules* 9 (2004) 815.
- [13] P. Roy, M. Manassero, *Dalton Trans.* 39 (2010) 1539.
- [14] D. Maiti, J.S. Woertink, A.A.N. Sarjeant, E.I. Solomon, K.D. Karlin, *Inorg. Chem.* 47 (2008) 3787.
- [15] T. Suksrichavalit, S. Prachayasittikul, C. Nantasenamat, C. Isarankur, N. Ayudhya, V. Prachayasittikul, *Eur. J. Med. Chem.* 44 (2009) 3259.
- [16] M. Barba, A.P. Sobolev, C. Romeo, E. Schinina, D. Pietraforte, L. Mannina, G. Musci, F. Polticelli, *Protein Sci.* 18 (2009) 559.
- [17] S.M. Berry, *J. Biol. Inorg. Chem.* 14 (2009) 143.
- [18] A.S. El-Tabl, S.A. El-Enein, *J. Coord. Chem.* 57 (2004) 281.
- [19] R. Franski, T. Kozik, B. Staniszewski, W. Urbaniak, *Eur. J. Chem.* 8 (2010) 508.
- [20] N. Le Moan, G. Clement, S. Le Maout, F. Tacnet, M.B. Toledano, *J. Biol. Chem.* 281 (2006) 15.
- [21] H.M. Marafie, H.B. Youngo, M.S. El-Ezaby, *J. Coord. Chem.* 56 (2003) 579.
- [22] X. Qjiao, Z.Y. Ma, C.Z. Xie, F. Xue, Y.W. Zhang, J.Y. Xu, Z.Y. Qiang, J.S. Lou, G.J. Chen, S.P. Yan, *J. Inorg. Biochem.* 105 (2011) 728.
- [23] K.S. Kumar, S. Ganguly, R. Veerasamy, E. De Clercq, *Eur. J. Med. Chem.* 45 (2010) 5474.
- [24] S.E.H. Etaiw, D.M. Abd El-Aziz, E.H. Abd El-Zaher, E.A. Ali, *Spectrochim. Acta, Part A* 79 (2011) 1331.
- [25] Z. Travnicek, M.M. Matikova, R. Novotna, *J. Inorg. Biochem.* 105 (2011) 937.
- [26] P.K. Panchal, H.M. Parekh, P.B. Pansuriya, *J. Enzyme Inhib. Med. Chem.* 21 (2006) 203.
- [27] A. Kumari, I. Singh, J.P. Tandon, *Appl. Organomet. Chem.* 9 (1995) 127.
- [28] M. Rodriguez, G. Ramos-Ortiz, J.L. Maldonado, V.M. Herrera-Ambroz, O. Dominguez, R. Santillan, N. Farfan, K. Nakatani, *Spectrochim. Acta, Part A* 79 (2011) 1757.
- [29] M. Nath, P.K. Saini, *Dalton Trans.* 40 (2011) 7077.
- [30] B. Kosar, Ç. Albayrak, *Spectrochim. Acta, Part A* 78 (2011) 160.
- [31] A. Trujillo, F. Justaud, L. Toupet, O. Cadot, D. Carrillo, C. Manzur, J.R. Hamon, *New J. Chem.* 35 (2011) 2027.
- [32] F. Robert, A.D. Naik, F. Hidara, *Eur. J. Org. Chem.* 4 (2010) 621.
- [33] G. Tomasello, G.G. Olaso, P. Altoe, *J. Am. Chem. Soc.* 131 (2009) 5172.
- [34] M.N. Chaur, D. Collado, J.M. Lehn, *Chem. Eur. J.* 17 (2011) 248.
- [35] M. Kraemer, M. Pita, J. Zhou, M. Ornatka, A. Poghosian, M.J. Schoning, E. Katz, *J. Phys. Chem. C* 113 (2009) 2573.
- [36] S. Menati, A. Azadbakht, R. Azadbakht, A. Taeb, A. Kakanejadifard, *Dyes Pigments* 98 (2013) 499.
- [37] H. Khanmohammadi, K. Rezaeian, M.M. Amini, S.W. Ng, *Dyes Pigments* 98 (2013) 557.
- [38] A.N.M.A. Alagha, H.A. Bayoumi, Y.A. Ammar, S.A. Aldhmani, *J. Mol. Struct.* 1035 (2013) 383.
- [39] C. Anitha, C.D. Sheela, P. Tharmaraj, S.J. Raja, *Spectrochim. Acta, Part A* 98 (2012) 35.
- [40] M. Aslantas, N. Kurtoglu, E. Sahin, M. Kurtoglu, *Acta Crystallogr., Sect. E* 634 (2007) o3637.
- [41] M. Köse, N. Kurtoğlu, Ö. Gümüşşu, D. Karakaş, M. Tutak, V. McKee, M. Kurtoğlu, *J. Mol. Struct.* 1053 (2013) 89.
- [42] Bruker (1998). *APEX2 and SAINT Bruker AXS Inc.*
- [43] G.M. Sheldrick, *Acta Crystallogr., Sect. A* 64 (2008) 112.
- [44] H. Khanmohammadi, M. Darvishpour, *Dyes Pigments* 81 (2009) 167.
- [45] D.H. Williams, I. Fleming, *Spectroscopic Methods in Organic Chemistry*, third ed., McGraw Hill, New York, 1980, p. 49.
- [46] F. Arslan, M. Odabaşoğlu, H. Ölmez, O. Büyükgüngör, *Polyhedron* 28 (2009) 2943.
- [47] B. Kosar, Ç. Albayrak, M. Odabasoglu, O. Büyükgüngör, *Int. J. Quantum Chem.* 111 (2010) 3654.
- [48] H. Khanmohammadi, M. Darvishpour, *J. Inorg. Organomet. Polym. Mater.* 21 (2011) 541.
- [49] G. Kurtoglu, B. Avar, H. Zengin, M. Kose, K. Sayin, M. Kurtoglu, *J. Mol. Liq.* 200 (2014) 105.